DMD Fast Forward. Published on August 22, 2018 as DOI: 10.1124/dmd.118.082636
This article has not been copyedited and formatted. The final version may differ from this version.

A Commentary: Finding T_{max} and C_{max} in Multi-Compartmental Models

Yi Rang Han, Ping I. Lee, and K. Sandy Pang

Department of Pharmaceutical Sciences, Leslie Dan Faculty of Pharmacy, University of Toronto, Toronto, Canada

DMD Fast Forward. Published on August 22, 2018 as DOI: 10.1124/dmd.118.082636
This article has not been copyedited and formatted. The final version may differ from this version.

Running title: T_{max} and C_{max} for multi-compartmental models

Corresponding author: K. Sandy Pang 144 College Street, Toronto, Ontario, M5S 3M2 Tel: 416-978-6164 Fax: 416-978-8511 Email: ks.pang@utoronto.ca

Abstract: 243 words

Introduction: 803 words

Methods: 2596 words

Discussion: 505 words

References: 16

Tables: 2

Figures: 6

DMD Fast Forward. Published on August 22, 2018 as DOI: 10.1124/dmd.118.082636
This article has not been copyedited and formatted. The final version may differ from this version.

List of Abbreviations

AUC: area under the blood/plasma concentration time curve

C: drug concentration in the blood/plasma (central) compartment

C_{max}: maximum concentration in blood/plasma

$C_{max,obs}$: maximum concentration observed among the blood/plasma sampling points

$C_{max,2comp}$: maximum blood/plasma concentration in (central) compartment from 2 compartment model fit

$C_{max,true}$: true maximum concentration reached in the blood/plasma (central) compartment

C_{SS}: steady-state drug concentration in the blood/plasma (central) compartment

$T_{max,true}$: true time needed to reach the maximum concentration in the blood/plasma (central) compartment

$T_{max,obs}$: time observed to reach the $C_{max,obs}$ in blood/plasma (central) compartment

$T_{max,2comp}$: time observed to reach the $C_{max,2comp}$ in the blood/plasma (central) compartment based on the two-compartment model

u: time elapsed since last dose in multiple dosing

$u_{max,SS}$: time (normalized to τ) to reach $C_{max,ss}$ concentration from last administered dose

τ: dosing interval in a multiple dosing regimen

α: hybrid constant for two-compartment model

β: hybrid constant for two-compartment model

V_1: Volume of central compartment

A_i: coefficient for an i^{th} compartment model

λ_i: hybrid constant for an i^{th} compartment model

k: elimination rate constant for one compartment model

k_a: first order absorption rate constant

F_{sys}: systemic oral bioavailability, product of fraction absorbed (F_{abs}) and availabilities of intestine, liver and lung from the first pass effect

$Dose_{po}$: oral dose administered

k_{21}: first order transfer rate from compartment 2 to 1 (used in both 2 and 3 compartment models)

k_{31}: first order transfer rate from compartment 3 to 1 (3 compartment model)

L: coefficient for two-compartment model corresponding to exponent α

M: coefficient for two-compartment model corresponding to exponent β

m: the number of compartments

N: coefficient for two-compartment model corresponding to exponent k_a

Ɛ: assay error

Abstract

Drug absorption data are critical in bioequivalence comparisons, and factors such as the maximum concentration (C_{max}), the time to achieve C_{max} (or T_{max}), as well as the area under the curve (AUC) are important metrics. It is generally accepted that the AUC is a meaningful estimate of the extent of absorption and T_{max} or C_{max} may be used for assessing the rate of absorption. But the estimation of the rate of absorption with T_{max} or C_{max} is not always feasible, as explicit solutions relating T_{max} and C_{max} to the absorption (k_a) and elimination rate (k) constants exist only for the one and not multi-compartment oral model. Therefore, the determination of T_{max} or C_{max} for multi-compartment models is uncertain. Here, we propose an alternate, numerical approach that uses the point-slope method for the first/second derivatives of the concentration vs. time profiles and the Newton Raphson iteration method for the determination of T_{max} and C_{max}. We show that the method holds for multi-compartmental oral dosing under single or steady-state conditions in the absence of known microconstants even for flip-flop ($k_a < \beta$) models. Simulations showed that the C_{max} and T_{max} estimates obtained with the Newton Raphson method were more accurate than those based on the noncompartmental, observation-based method recommended by the FDA. The %Bias due to sampling frequency and assay error were less than those determined by the noncompartmental method, showing that the Newton Raphson method is viable for the estimation of T_{max} and C_{max}.

DMD Fast Forward. Published on August 22, 2018 as DOI: 10.1124/dmd.118.082636
This article has not been copyedited and formatted. The final version may differ from this version.

INTRODUCTION

Drug absorption data are often utilized in bioequivalence comparisons. The FDA recommends two measures: the area under the curve (AUC) and the maximum concentration, C_{max}, (CDER/FDA, 2015), with AUC as the primary and C_{max} as the secondary measure. The AUC is known to be independent of k_a, the absorption rate constant under first-order conditions that reflects the extent of drug absorption, and this is normally calculated by the trapezoidal rule that is straightforward for both compartmental and noncompartmental models. The FDA defines C_{max} as the maximum concentration observed in the sampled blood or plasma data, and is henceforth denoted as $C_{max,obs}$. This $C_{max,obs}$ partly serves to provide insight into the rate of absorption. However, an understanding of the absorption rate is more complex. As previously noted (Endrenyi and Al-Sahikh, 1995; Basson et al., 1996), the C_{max} is affected by both the extent and the rate of absorption. In addition, the value of $C_{max,obs}$ is further influenced by the frequency of the sampling scheme and the magnitude of the assay errors. As the sampling frequency or assay error is increased, $C_{max,obs}$ is increased as well (Endrenyi and Al-Sahikh, 1995). Thus, the comparison between $C_{max,obs}$ values that are generated by two divergent sampling schemes or assaying methods may be inappropriate. An alternate measure of the absorption rate is the time to reach $C_{max,obs}$ or $T_{max,obs}$, which has been suggested to be an unconfounded metric for the rate of absorption (Basson et al., 1996). However, the $T_{max,obs}$ is a categorical variable, one that can take on a limited and usually fixed number of possible values and its discriminating power depends strongly again on the sampling frequency.

Generally speaking, values for C_{max} and T_{max} may be obtained by fitting data to compartmental models and then computing those values based on the fitted parameters. In the case of the one-compartment model, the model-guided determination of $T_{max,1comp}$ and $C_{max,1comp}$ is clear.

The concentration C_{1comp} may be expressed in terms of the absorption rate constant, k_a, and elimination rate constant, k, in a biexponential expression, as follows:

$$C_{1comp} = \frac{k_a F_{sys} Dose_{po}}{V_1(k_a - k)}\left[e^{-kt} - e^{-k_a t}\right] = A'\left[e^{-kt} - e^{-k_a t}\right] \quad (1)$$

where V_1 is the volume of the distribution and $A' = \frac{k_a F_{sys}\ Dose_{po}}{V_1(k_a - k)}$. The condition at $T_{max,1comp}$ yields the $C_{max,1comp}$.

$$C_{max,1comp} = \frac{k_a F_{sys}\ Dose_{po}}{V_1(k_a - k)}\left[e^{-kT_{max,1comp}} - e^{-k_a T_{max,1comp}}\right] \quad (1A)$$

Explicit solutions for $T_{max,1comp}$ is obtained by solving $dC_{1comp}/dt = 0$ (Eq. 2).

$$T_{max,1comp} = \frac{\ln(k_a/k)}{k_a - k} \quad (2)$$

The rate constant, k_a, may be estimated via curve stripping or with the Wagner-Nelson method (Wagner and Nelson, 1963) to obtain the fraction remaining to be absorbed (FRA), $FRA = \frac{(A_A)_\infty - (A_A)_T}{(A_A)_\infty} = e^{-k_a t}$. Together with k and $\frac{k_a F_{sys} Dose_{po}}{V_1(k_a - k)}$, $C_{max,1comp}$ and $T_{max,1comp}$ may be calculated (Eqs. 1 and 2). The equation holds in the case of flip-flop when $k_a < k$.

The one compartment analytical equation for finding T_{max} and C_{max} can be extended to scenario with absorption lag time. This may be derived by substituting the observed time $(t + t_{lag})$ and then solving the analogous problem of the form, $dC_{1comp,lag}/dt = 0$ in Eq. 2. The one-compartment concentration profile is:

$$C_{1comp,lag} = \frac{k_a F_{sys} Dose_{po}}{V_1(k_a - k)}\left[e^{-k(t-t_{lag})} - e^{-k_a(t-t_{lag})}\right] \quad (3)$$

and the associated T_{max} is:

$$T_{max,1comp,lag} = \frac{\ln(k_a/k)}{k_a - k} + t_{lag} \quad (4)$$

For the two-compartmental model, a triexponential expression now describes the drug concentration with oral dosing (Gibaldi and Perrier, 1982):

$$C = Ne^{-k_a t} + L\,e^{-\alpha t} + M\,e^{-\beta t}$$

$$\text{where } N = \frac{k_a F_{sys} Dose_{po}(k_{21} - k_a)}{V_1(\alpha - k_a)(\beta - k_a)}\ ;\quad L = \frac{k_a F_{sys} Dose_{po}(k_{21} - \alpha)}{V_1(k_a - \alpha)(\beta - \alpha)};\quad M = \frac{k_a F_{sys} Dose_{po}(k_{21} - \beta)}{V_1(k_a - \beta)(\alpha - \beta)} \quad (5)$$

An accurate estimation of the parameters is more complex for such a triexponential expression reserved for the two-compartment, oral case (Eq. 5), and several scenarios are possible. First is when $k_a >> \beta$, and the 3 exponential components are easily and accurately separated upon curve stripping (Gibaldi and Perrier, 1982). With known k_{12}, k_{21}, k_{10} and V_1 from intravenous (iv) dosing, k_a can be obtained by the Loo-Riegelman method (Loo and Riegelman, 1968) with the usual assumption that elimination occurs in the central compartment. However, for cases when $\beta >$ or $\approx k_a$, the distinguishing feature of a prominent "hat" or "nose" that occurs with rapid absorption and slow elimination now disappears, and the oral profile shrinks to one resembling that for the one-compartment model (Chan and Gibaldi, 1985). Under this circumstance, the k_a so obtained by the curve stripping procedure is no longer accurate. Even if the parameters for the two-compartment model can be accurately determined, the analysis of T_{max} and C_{max} in drugs that exhibit multiple compartmental characteristics, however, cannot be solved explicitly. Often, the Loo-Riegelman method (Loo and Riegelman, 1968) is used first to obtain k_a, then C_{max} and T_{max}, but the

DMD Fast Forward. Published on August 22, 2018 as DOI: 10.1124/dmd.118.082636
This article has not been copyedited and formatted. The final version may differ from this version.

microconstants, k_{12}, k_{21}, and k_{10}, and the assumption that elimination occurs from the central compartment are required.

In this communication, we demonstrated the use of a numerical approach for the model-guided determination of T_{max} and C_{max} in multi-compartment models, and compared the estimates so obtained to those from direct observations ($T_{max,obs}$ and $C_{max.obs}$), a method encouraged by regulatory agencies such as the FDA. This method utilizes the second derivative of the concentration vs. time and the point slope and Newton Raphson method. The bias due to assay error and sampling frequency, as well as its performance for different k_a values are discussed.

THEORY AND METHODS

Finding T_{max} and C_{max} in multicompartment models

The C_{max} and T_{max} for oral dosing for a two-compartment may be found in a manner similar to that described for the one-compartment. The $C_{max,2comp}$ occurs when the first derivative (Eq. 6) is zero.

$$\frac{dC_{2comp}}{dt} = N(-k_a)e^{-k_a t} + L(-\alpha)e^{-\alpha t} + M(-\beta)e^{-\beta t} = 0 \text{ at } T_{max,2comp} \quad (6)$$

The above problem may be solved numerically using the Newton-Raphson method (Galantai, 2000), since the second derivative, $(\frac{d^2C_{2comp}}{dt^2})$ may be easily computed:

$$\frac{d^2C_{2comp}}{dt^2} = Nk_a^2e^{-k_a t} + L\alpha^2e^{-\alpha t} + M\beta^2e^{-\beta t} \quad (7)$$

We will illustrate the solution with examples, first with the two-compartment model, then with multi-compartmental models, for drugs with a fast vs. a slow absorption rate constant.

Example 1: oral dosing for the two-compartment model drugs

The following example demonstrates use of this method to obtain $C_{max,2comp}$ and $T_{max,2comp}$. The following parameters were selected for the scenario of fast vs. slow absorption: $k_a = 2$ (fast) or 0.1 (slow) h^{-1}, with common values for $\beta = 0.2\ h^{-1}$, $\alpha = 0.8\ h^{-1}$, $k_{21} = 0.5\ h^{-1}$ and $F_{sys}Dose_{po}/V_1 = 100$. Microconstants k_{10}, k_{12}, and k_{21} will remain unchanged when β, α, and k_{21} are kept constant, due to the relations that exist between α, β, k_{10}, k_{12}, and k_{21} ($\alpha*\beta = k_{10}*k_{21}$ and $\alpha+\beta = k_{12}+k_{10}+k_{21}$). In fact, the hybrid constants correspond to k_{10}, k_{12}, and k_{21} values of 0.32, 0.18, and 0.5 h^{-1}, respectively. After substitution of the selected values into Eq. 5, values of the drug concentration, C_{2comp}, in the central compartment, the derivatives, $\frac{dC_{2comp}}{dt}$, $\frac{d^2C_{2comp}}{dt^2}$, and the $T_{max,2comp}$ estimates were computed and summarized in Table 1. The concentration-time profile and the two-compartmental model are shown in Figure 1A showing a prominent "nose", and components of absorption (k_a), distribution (α) and elimination (β) for fast absorption, or an apparent one compartment profile for slow absorption (Figure 2A). For fast absorption, the k_a may be obtained by the method of residuals. However, for slow absorption (Figure 2A), k_a may only be estimated with the Loo and Riegelman method (Loo and Riegelman, 1968) when the microconstants k_{12}, k_{21}, and k_{10} are known. In contrast, for both fast and slow absorption, the Newton Raphson method (Galantai, 2000) may be used to obtain $T_{max,2comp}$ without the knowledge of the microconstants.

Fast k_a. A time-expanded view of Figure 1B showed that the dC_{2comp}/dt profile intersected at the zero line (obtained when Eq. 6 =0), then continued negatively before rebounding upwards, rising asymptotically to parallel and approach 0. The first derivative (in inset), when set = 0 in Eq. 6, provided the $T_{max,2comp}$ estimate, which equaled 0.97 h graphically from the inset (see value in Table 1). Such a fast absorption can occur in the case of immediate release oral dosage forms of morphine

and cefaclor (Barbhaiya *et al.*, 1990; Collins *et al.*, 1998). Even faster T_{max} is possible for bolus subcutaneous routes of morphine and other drugs (Home *et al.*, 1999; Stuart-Harris *et al.*, 2000), for which the method presented here is also applicable.

The iterative scheme of the Newton Raphson method to find where the function is zero is illustrated in detail in Figure 1B. An initial time estimate ($T_{estimate1}$) is required for the numerical method. For demonstration purposes, an arbitrary time of 0.25 h was selected for ($T_{estimate1}$). For practical applications, $T_{max,obs}$ may be used as the initial estimate for $T_{estimate1}$. At $T_{estimate1}$, the tangent line of the function dC_{2comp}/dt was constructed using the "point-slope method", where the slope was essentially $\frac{d^2C_{2comp}}{dt^2}$ evaluated at $T_{estimate1.}$ From the line equation of the tangent (y = mx+b), the x-intercept at y=0 (i.e. the time value a_1) was computed, yielding the corresponding $T_{estimate2}$ on the dC_{2comp}/dt curve (see Figure 1B, green). The point-slope procedure was repeated as shown in the blue point in Figure 1B to provide a_2 and the 3rd estimate, ($T_{estimate3}$). The continued iterations lead to $T_{estimatei}$ value for which the difference between dC_{2comp}/dt and 0 is less than a chosen tolerance level (ε). When this criterion is met, the numerical method has converged to $T_{max,true.}$

Convergence may be achieved numerically in the critical point that may not be of interest. We illustrate this with the scenarios below in Figure 1C, which shows the behavior of the dC_{2Comp}/dt vs. time curve in a more expanded time scale. When the initial $T_{estimate1}$ (within the shaded green region) was appropriately selected before the minimum for the dC_{2comp}/dt curve (at 1.9 h, or the boundary between shaded green and red regions in Figure 1C), one would obtain the true $T_{max,2comp,true}$ at convergence. However, if the initial $T_{estimate1}$ was selected from the red zone (Figure 1C), the numerical method would not converge to $T_{max,2comp,true}$. Hence, it is important to select an appropriate value for $T_{estimate1}$. For good initial estimates between 0 and 1.9 h (where $\frac{d^2C_{2comp}}{dt^2}$ is 0

in Figure 1C, with the $T_{max,2comp,true}$ at 0.97 h), the numerical method would converge and yield the true $T_{max,2comp}$ value at the minimum. Estimates larger than 1.9 h, however, may lead to the asymptotic value of 0 (Figure 1C). When all the $T_{estimate}$ values are plotted on the C vs. time plot (shown as differently colored points in inset of Figure 1A), it may be seen that the estimates readily approach $T_{max,2comp,true}$. With known $T_{max,2comp,true}$, the corresponding $C_{max,2comp,true}$ may be calculated (Eq. 5).

Slow k_a. By contrast, the concentration profile and the two-compartmental model with slow k_a, shown in Figure 2A, revealed an apparent, one-compartment characteristic. The absorption constant (k_a) could be obtained only with the Loo and Rigelman (1968) method with known microconstants, k_{12}, k_{21}, and k_{10}, or simultaneously curve fitting with intravenous data involving these microconstants. Again, the iterative Newton Raphson method could be readily applied here. By selecting $T_{estimate1}$, finding a_1 then $T_{estimate2}$, the point-slope procedure was applied to provide a_2 and $T_{estimate3}$, then eventually $T_{max,2comp,true}$ (Figure 2C, showing comparable green and red regions as in Figure 1C), similar to the iteration scheme of Figure 1 when k_a is faster (2 h^{-1}). The only difference now was that the procedure provided a "shallow well" when $\frac{d^2C_{2comp}}{dt^2}$ was set = 0 in Eq. 7 (Figure 2C). The first derivative (Figure 2C), when set = 0, revealed the true $T_{max,2comp}$ estimate of 5.8 h^{-1}. The points on C_{2comp} vs. time plot (Figure 2A) showed the progression in approaching the true $C_{max,2comp}$ and $T_{max,2comp}$ when k_a is slow (0.1 h^{-1}). Again, when the initial $T_{estimate1}$ (within the shaded green region, Figure 2C) was appropriately selected before the minimum for the dC_{2comp}/dt curve (at 12.5 h, or boundary between shaded green and red regions in Figure 2C), then one would obtain the true $T_{max,2comp,true}$ at convergence. For good initial estimates between 0 and 12.5 h (where $\frac{d^2C_{2comp}}{dt^2}$ is 0 in Figure 2C, with the $T_{max,2comp,true}$ at 5.77 h), the numerical method would converge

and yield the true $T_{max,2comp}$ value at the minimum. Initial estimates larger than 12.5 h, however, may lead to the asymptotic value of 0 (Figure 2C). Long T_{max}'s have been observed for the slow, oral absorption profiles of drugs such as sertraline (> 7 h) (Allard et al., 1999) and zonisamide (5-6 h) (Mimaki, 1998).

Figures 1 and 2 both illustrate that the Newton Raphson method works well regardless whether $k_a > \beta$, or $k_a < \beta$.

Example 2: oral dosing for multi-compartment model drugs

The general method is applicable not only to examine temporal data after single oral dosing for the two-compartment model cases, but also for multiple dosing at steady-state. The concentration for multicompartmental models is shown below, whose hybrid constants are denoted as λ_i

$$C = A_a e^{-k_a t} + \sum_{i=1}^{m} A_i e^{-\lambda_i t} \quad (8)$$

To demonstrate this, a three-compartment, single oral dosing model, with elimination from central compartment, was simulated for case where $k_a > \lambda_i$ and $k_a < \lambda_i$. The selected values are summarized in Table 1, with the method for estimation of $T_{max,3comp}$ the same as that for the two-compartment model (see Figure 3). With known $T_{max,3comp,true}$, the corresponding $C_{max,3comp,true}$ may be calculated.

Extension of the Newton Raphson method for estimating T_{max} in multiple dosing

DMD Fast Forward. Published on August 22, 2018 as DOI: 10.1124/dmd.118.082636
This article has not been copyedited and formatted. The final version may differ from this version.

The method may be readily applied to multiple dosing at steady-state, as exemplified below for the two-compartment model, where u is the time elapsed after the last dose here. The domain of the numerical problem is $0 \le u \le \tau$, where τ is the interval of administration.

$$C_{2comp,SS} = N\left(\frac{1}{1-e^{-k_a\tau}}\right)e^{-k_a u} + L\left(\frac{1}{1-e^{-\alpha\tau}}\right)e^{-\alpha u} + M\left(\frac{1}{1-e^{-\beta\tau}}\right)e^{-\beta u} \quad (9)$$

$C_{max,2comp,SS}$ occurs at $u_{max,2comp,SS}$, the true $T_{max,2comp}$ or $T_{max,2comp,true}$ after the last dose can be computed by solving $\frac{dC_{2comp,SS}}{du} = 0$.

$$\frac{dC_{2comp,SS}}{du} = \left(\frac{-k_a N}{1-e^{-k_a\tau}}\right)e^{-k_a u} + \left(\frac{-\alpha L}{1-e^{-\alpha\tau}}\right)e^{-\alpha u} + \left(\frac{-\beta M}{1-e^{-\beta\tau}}\right)e^{-\beta u} = 0 \quad (10)$$

Here, the value of u, which satisfies the condition for Eq. 11 (shown below), occurs at $u_{max,SS}$, the time elapsed since last dose where maximum concentration ($C_{max2comp,SS}$) occurs, in the steady state.

This method may be extended to multi-compartment multiple dosing systems whose steady state concentration with dosing interval of τ is given by:

$$C_{SS} = A_a\left(\frac{1}{1-e^{-k_a\tau}}\right)e^{-k_a u} + \sum_{i=1}^{m} A_i\left(\frac{1}{1-e^{-\lambda_i\tau}}\right)e^{-\lambda_i u} \quad (11)$$

An example of the calculation is shown for the 2 and 3 compartments in Figure 4, and detailed parameter values are summarized in Table 1. The method for estimation of $T_{max,multi,true}$ is the same as that for all other models described above.

Simulations

Simulations were performed to assess the properties of the proposed method, and compare this to non-compartmental analysis, where C_{max} and T_{max} are based directly on the observed data.

DMD Fast Forward. Published on August 22, 2018 as DOI: 10.1124/dmd.118.082636
This article has not been copyedited and formatted. The final version may differ from this version.

The pharmacokinetic parameters used in the previous 2-compartment model: α, β, and k_{21} of 0.8, 0.2 and 0.5 h^{-1}, respectively, were applied here. $F_{sys}Dose_{po}/V_1$ was set to 100. Blood concentration data were simulated using the commercial software (MATLAB, The MathWorks Inc., Natick, MA) for the two-compartment, oral model, with elimination in central compartment. The designated hybrid (α and β) and k_a and k_{21} values were used to compute N, L, and M with Eq. 5 and then used to provide values of $C_{2comp,cal}$ for each of the designated sampling times. We compared between the non-compartmental method via visual identification and our method under different assay errors and sampling frequencies. Simulations were repeated 500 times and accuracy and precision of the two estimated metrics (X = C_{max} or T_{max}) each acquired through two different methods were evaluated by computing bias and relative standard deviation. %Bias, which is the deviation of the mean value ($\bar{x}$) from true value (x_{true}), was calculated using Eq. 12.

$$\%\text{Bias} = \frac{\bar{x} - x_{true}}{x_{true}} \times 100\% \tag{12}$$

The relative standard deviation (RSD) of the repeat simulations was calculated using Eq. 13, where x_i is the estimated metric for each of the repeats and $\bar{x}$ is the mean of the estimates and N is the number of replicate simulations (N = 500).

$$RSD = \sqrt{\sum_i \frac{x_i - \bar{x}}{N-1}} \times \frac{1}{\bar{x}} \tag{13}$$

Assay Error. To understand the effect of assay error, simulations were performed using conditions similar to that proposed by Tothfalusi and Endrenyi (2003). The sampling time was set to a geometric sequence, starting at 0.05 and with a geometric ratio of 1.3 for a total of 24 time points. For the two-compartment model with elimination from the central compartment, k_a was set to be 2

DMD Fast Forward. Published on August 22, 2018 as DOI: 10.1124/dmd.118.082636
This article has not been copyedited and formatted. The final version may differ from this version.

h^{-1}. Then, Gaussian noise, with a mean of 0 and relative standard deviation of $\frac{Ɇ}{100} * C_{2comp,cal}$ (where $C_{2comp,cal}$ is the error-free value and Ɇ is the assay error, 1-15%) was generated to simulate error-containing concentrations ($C_{2comp,error}$) among the 500 simulations for each of the 5 designated assay errors (1, 2, 5, 10, and 15%). The parameters, $T_{max,2comp}$ and $C_{max,2comp}$, were obtained directly from N, L, and M, k_a, α, and β, with the set of $C_{2comp,error}$ (with error) data from nonlinear fitting of the two-compartment model using Matlab, which provided a solution for the constants, N, L, M, k_a, α and β. These fitted estimates were substituted into Eq. 6 and Newton Raphson numerical method was performed to solve the resulting expression. The non-compartmental $T_{max,obs}$ was used as the initial estimate. In cases where proper convergence was not achieved, the previous time point to $T_{max,obs}$ was used as the initial estimate and the numerical analysis was repeated. The analysis yielded $T_{max,2comp}$ and $C_{max,2comp}$ for comparison with their counterparts in the absence of assay error, $T_{max,2comp,true}$ and $C_{max,2comp,true}$. Alternately, the parameters may be used to simulate concentrations at small incremental time intervals to arrive at C_{max} estimates close to the $C_{max,2comp,true}$. The maximum concentration, $C_{max,2comp,true}$, and its corresponding time, $T_{max,2comp,true}$, were then identified visually.

The %Bias and relative standard deviation values of $C_{max,2comp}$ (Figures 5A and 5C) and $T_{max,2comp}$ (Figures 5B and 5D) due to assay error from our proposed model-guided estimation method were much smaller than those from the noncompartmental method, which is based merely on visual inspection of the observed data for $C_{max.2comp,obs}$ and $T_{max,2comp,obs}$. Essentially, there was little bias on $C_{max,2comp}$ and $T_{max,2comp}$ for our model-guided estimation method, whereas for the noncompartmental method, the %Bias for $C_{max,2comp,obs}$ was higher and proportional to the assay error (Figure 5A). Thus, $C_{max,2comp}$ values obtained from datasets with different assay errors cannot

be compared reliably when using the noncompartmental method, while the compartmental model-guided values allow for comparison across different studies.

***Sampling Frequency*.** Next, to evaluate the impact of sampling the frequency, 500 simulations were performed for each for the four sampling frequencies ranging from 5, 10, 20 and 40. The sampling frequency reflects the number of sampling points between 0 and $T_{max,2comp,true}$, allowing the true $T_{max,2comp}$ to fall on one of the sampling times. Again, the hypothetical patient data were simulated with the assigned set of $k_a, k_{21}, \alpha,$ and β values assuming elimination from the central compartment, a specific blood sampling scheme, and a constant 5% assay error. This data were refitted by nonlinear least squares method to obtain the parameters $N, L, M, k_a, \alpha,$ and β, such that the $C_{max,2comp,true}$ and $T_{max,2comp,true}$ could be obtained with the Newton Raphson method, as previously described.

Even as the sampling frequency was increased, $C_{max,2comp}$ obtained by our method (Figure 6A) showed no apparent bias, in contrast to the FDA recommended method, which showed positive bias. Furthermore, the degree of bias increased as sampling frequency was increased, suggesting that C_{max} cannot easily be compared between datasets that were generated using different sampling frequencies. The positive bias for the visual inspection method is at first counter-intuitive since in the absence of assay errors, C_{max} should have negative bias as by definition all other concentration values are equal or lower. However, due to presence of assay errors, the measured concentrations near the true $C_{max,true}$ may be greater than $C_{max,true}$ and since the non-compartmental method based on visual inspection selects the largest concentration, positive bias occurs on average.

In addition, both $T_{max,2comp}$ and $C_{max,2comp}$ can be obtained with more certainty (lower relative standard deviation) using our method than when obtained directly from the measurements

(Figures 6C and 6D). Because population variation was not added to the data, the variation measured here arose from the assay errors and the sampling scheme. Figure 6B shows that the $T_{max,2comp}$ obtained using the two methods show only minor bias. The small positive bias shown here is due to the asymmetric peak shape near $T_{max,true}$ (ie. peak is sharper in the left region than the right region). As previously noted (Basson et al., 1996), measuring $T_{max,2comp}$ is a universal method and the $T_{max,2Comp}$ may be used also under flip-flop kinetics, for which separation of k_a may be difficult without intravenous data. However, the determined $T_{max,2comp}$ suffers from a higher relative standard deviation when compared to $C_{max,2comp}$ (Figures 6C and 6D).

k_a. The influence of k_a on the $T_{max,2comp}$ and $C_{max,2comp}$ estimates and the applicability of the method were appraised using simulations with five different k_a values: 3, 2, 1, 0.1, and 0.05 h^{-1} (Table 2). The sampling times were made between 0.025 and 48 h (at 0.025, 0.05, 0.1, 0.25, 0.75, 1, 1.5, 2, 2.5, 3, 4, 6, 8, 12, 18, 24, 30, 36, 42 and 48 h) with an assay error of 5% (i.e., Assay error ₱ = 5). The method was found to be applicable to cases where $k_a > \beta$ and $k_a < \beta$. For all k_a values, the RSD was lower for the 2 compartmental fitting-based method, and varied between 2.19% and 5.78% in contrast to the noncompartmental method whose RSD varied between 3.76% and 23.3% (Table 2).

DISCUSSION

Generally speaking, the model-guided estimation method proposed here using the Newton Raphson method requires additional analysis in comparison to noncompartmental analysis. The Newton-Raphson numerical method was implemented from scratch and the estimates would converge well when the $T_{max,obs}$ is used as initial estimates. Moreover, in various mathematical software applications, zero-finding methods are available as built-in functions (for example, fzero in the case of Matlab). Not all of these use the Newton-Raphson method, but the functions utilized

are adequate in solving the zero-finding problem numerically (i.e,, f(x)=0 problem). Despite the small amount of added work compared to the non-compartmental analysis method, the model guided analysis provides reduced bias for the determination of C_{max} (Table 2, Figures 5A and 6A) and is associated with a higher precision in the determination of both C_{max} (Figures 5C and 6C) and T_{max} (Figures 5D and 6D). Moreover, in this analysis, we have not considered the C_{max} at fast burst effect of the drug at t=0, when the burst behaves like an IV bolus, due to the accompanying complexities.

In contrast to the Loo-Riegelmen method (Loo and Riegelman, 1968), the model-guided estimation method proposed here does not assume a detailed mechanistic model nor require microconstants, making it suitable even when intravenous data are not available. In addition, our method may be used to analyze data under flip-flop kinetics; this is demonstrated by the example with $k_a < \beta$ (Figure. 2). In fact, our method is applicable generally to all multi-compartmental models that are approximated as sum of exponentials under linear conditions. While the number of exponentials is required, explicit knowledge of the detailed compartmental scheme is not required.

One disadvantage of our method is that bias may be introduced when inappropriate number of exponentials is selected. In cases where the constants are close in values, that is, $k_a \approx \alpha$ or $k_a \approx \beta$, the correct number of compartments will likely be underestimated, and $T_{max,true}$ is estimated with increased bias, albeit modest. Under the condition that $k_a = \alpha$ or when $k_a = \beta$, the accurate identification of the $T_{max,true}$ is not hampered and may be estimated without bias although we may be underestimating the number of compartments (data not shown). However, when the exponents are sufficiently separated the appropriate number of exponentials will be easily selected, and the model-guided interpolation will provide a lower bias on the C_{max} estimate and a higher precision for C_{max} and T_{max}. Hence, the method is viable for mostly all scenarios. Furthermore, this method

may be used even without intravenous data or a priori knowledge about the rank order of the hybrid constants α, β, and k_a. Thus, the model guided estimation method is appropriate for analyses comparing across aggregated datasets available from various sources, with varying collection parameters and limited mechanistic knowledge about the system.

Conclusion: A proper multiexponential fit, combined with the Newton Raphson method, can provide a better approach for C_{max} and T_{max} estimates than the observational, non-compartmental analysis method recommended by FDA, and is more appropriate when limited data are available.

Acknowledgements

Authorship Contributions

Participated in research design: Han, Pang

Conducted experiments: Han

Contributed new reagents or analytic tools: Han

Performed data analysis: Han

Wrote or contributed to the writing of the manuscript: Han, Lee, Pang

Conflicts: none

References

Allard A, Sainati SM, Roht-Schechter BF (1999) Coadministration of short-term zolpidem with sertraline in healthy women. *J Clin Pharmacol* **39**:184-191

Barbhaiya RH, Shukla UA, Gleason CR, Shyu WC, and Pittman KA (1990) Comparison of the effects of food on the pharmacokinetics of cefprozil and cefaclor. *Antimicrob Agents Chemother* **34**:1210–1213.

Basson RP, Cerimele BJ, DeSante KA, and Howey DC (1996) T_{max}: an unconfounded metric for rate of absorption in single dose bioequivalence studies. *Pharm Res* **13**:324-328.

CDER/FDA (2015) Guidance for Industry, Waiver of in vivo bioavailability and bioequivalence studies for immediate release solid oral dosage forms based on a biopharmaceutics classification system. *Cent Drug Eval Res* 1–2.

Chan KK, and Gibaldi M (1985) Assessment of drug absorption after oral administration. *J Pharm Sci* **74**:388–93.

Collins SL, Faura CC, Moore RA, and McQuay HJ (1998) Peak plasma concentrations after oral morphine: A systematic review. *J Pain Symptom Manage* **16**:388–402.

Endrenyi L, and Al-Sahikh P (1995) Sensitive and specific determination of the equivalence of absorption rates. *Pharm Res* **12**:1856–1864.

Galantai A (2000) The theory of Newton's method. *J Comput Appl Math* **124**:25–44.

Gibaldi M, and Perrier D (eds) (1982) *Pharmacokinetics*, 2nd ed., CRC Press.

Home PD, Barriocanal L, and Lindholm A (1999) Comparative pharmacokinetics and pharmacodynamics of the novel rapid-acting insulin analogue, insulin aspart, in healthy

volunteers. *Eur J Clin Pharmacol* **55**:199–203.

Loo JCK, and Riegelman S (1968) New method for calculating the intrinsic absorption rate of drugs. *J Pharm Sci* **57**:918–928.

Mimaki T (1998) Clinical pharmacology and therapeutic drug monitoring of zonisamide. *Ther Drug Monit* **20**:593-7.

Stuart-Harris R, Joel SP, McDonald P, Currow D, and Slevin ML (2000) The pharmacokinetics of morphine and morphine glucuronide metabolites after subcutaneous bolus injection and subcutaneous infusion of morphine. *Br J Clin Pharmacol* **49**:207–214.

Tothfalusi L, and Endrenyi L (2003) Estimation of C_{max} and T_{max} in populations after single and multiple drug administrations. *J Pharmacokinet Pharmacodyn* **30**:363–385.

Wagner JG (1975) Application of the Loo-Riegelman absorption method. *J Pharmacokinet Biopharm* **3**:51–67.

Wagner JG, and Nelson E (1963) Per cent absorbed time plots derived from blood level and/or urinary excretion data. *J Pharm Sci* **52**:610–611.

Figure Legends

Figure 1. The log-linear blood/plasma concentration versus time plot for a **two-compartment** oral dosing case, with elimination from central compartment, for drugs exhibiting fast absorption with $\mathbf{k_a}$ **of 2** $\mathbf{h^{-1}}$ and $> \beta$. Parameter values were: $\alpha, \beta,$ and k_{21}, are 0.8, 0.2, and 0.5 h^{-1}, respectively. (A) The dashed line is an extrapolated log linear terminal slope, β; the method of residuals would further provides α and k_a. The inset shows an expanded, zoomed-in version. (B) Plot of the first derivative vs. time with the first two iterations or $T_{estimate}$ are highlighted in green and blue; the inset shows the zoomed-out version of the same plot. A total of five iterations were required and these were replotted on Fig. 1A and the inset; see text for details], and (C) an expanded time plot of (Fig. 1B). Initial estimates, when chosen from the green and not red region in (C), highlights that the Newton-Raphson method will converge to the true or correct value. However, initial estimates chosen from the red region will not converge but approach infinity upon reaching the iteration limit.

Figure 2. The log-linear blood/plasma concentration versus time plot for a **two-compartment** oral dosing case, with elimination from central compartment, for drugs exhibiting flip-flop kinetics (slow absorption $\mathbf{k_a = 0.1\ h^{-1}} < \beta$). Parameter values were: $\alpha, \beta,$ and k_{21}, are 0.8, 0.2, and 0.5 h^{-1}, respectively, and values for $\alpha, \beta,$ and k_{21} were identical to those for Figure 1. (A) The colored square symbols are the iteration points of the Newton Raphson method; a zoomed-in plot is shown in the inset. (B) Plot of the first derivative as a function of time; In (B), the green and blue symbols are points used to obtain the first two iterations of the Newton Raphson method (see text for details). (C) shows the zoomed-out version of the same plot. Initial estimates made within the green but not red shaded region highlights where Newton-Raphson method will converge to correct value.

Figure 3. The log-linear blood/plasma concentration versus time plot for the **three-compartment** oral dosing, with elimination from central compartment. The right panel shows the derivative

dC_{3comp}/dt plot. The method is similar to that described for the two-compartment model. Parameter values for $\lambda_1, \lambda_2, \lambda_3, k_{21}$ and k_{31} are $1.0, 0.8, 0.2, 1.5,$ and $0.5\ h^{-1}$, respectively, with k_a of 2 h^{-1} (A) or 0.1 h^{-1} (B). The square symbols are the evaluation points used for computation of dC_{3comp}/dt by the Newton Raphson method; these same points also appeared in the right panels of (A) and (B). The squares are the evaluation points, and the method is similar to that described for the two-compartment model cases (see Figures 1 and 2).

Figure 4: The log-linear blood/plasma concentration vs. time plot for (A) two-compartment and (B) three compartment, multiple dosing. The dosing interval (τ) is 6 h. All other parameters for (A) are identical to those from Figure 1. All other parameters for (B) is identical to that shown in Figure 3A.

Figure 5. Plots of %Bias for C_{max} (A) or T_{max} (B) and the relative standard deviation or RSD (%) for C_{max} (C) or T_{max} (D) due to ***assay error*** for the noncompartmental method (blue square and line) - determined by non-compartmental analysis by direct observation and by model guided determination (red triangles and line) for two-compartment model.

Figure 6. Plots of %Bias for C_{max} (A) or T_{max} (B) and the relative standard deviation or RSD (%) for C_{max} (C) or T_{max} (D) due to ***sampling frequency*** for the noncompartmental method (blue square and line) - determined by non-compartmental analysis by direct observation and by model guided determination (red triangles and line) for two-compartment model. The sampling frequency is the number of sampling points between 0 and $T_{max,2comp,true}$. The parameters were same as that shown in Figure 1.

Table 1: Results (error free; assay error $E = 0$) arising from the Newton Raphson method for estimating of T_{max} from 2 or 3 compartmental models

Two-Compartment, oral (α = 0.8 h^{-1}, β = 0.2 h^{-1}; k_{21}= 0.5 h^{-1} ; $F_{sys}Dose_{po}/V_1$ = 100)		
	Fast Absorption (k_a = 2 h^{-1})	**Slow Absorption (k_a = 0.1 h^{-1})**
C_{2comp}	$-139e^{-2t} + 83.3e^{-0.8t} + 55.6e^{-0.2t}$	$57.1e^{-0.1t} - 7.14e^{-0.8t} - 50.0e^{-0.2t}$
dC_{2comp}/dt	$278e^{-2t} - 66.7e^{-0.8t} - 11.1e^{-0.2t}$	$-5.71e^{-0.1t} + 5.71e^{-0.8t} + 10.0e^{-0.2t}$
d^2C_{2comp}/dt^2	$-556e^{-2t} + 53.3e^{-0.8t} + 2.22e^{-0.2t}$	$0.571e^{-0.1t} - 4.57e^{-0.8t} - 2.00e^{-0.2t}$
$T_{max,2comp,true}$ (h)	0.972	5.57
$C_{max,2comp,true}$ (µg/mL)	64.2	163
Three-Compartment, oral (λ_1 = 1.0 h^{-1}; λ_2 = 0.8 h^{-1}; λ_3 = 0.2 h^{-1}; k_{21} = 0.5 h^{-1}; k_{31} = 1.5 h^{-1})		
	Fast Absorption (k_a = 2 h^{-1})	**Slow Absorption (k_a = 0.1 h^{-1})**
C_{3comp}	$-69.4e^{-2t} - 312e^{-1.0t} + 292e^{-0.8t} + 90.3e^{-0.2t}$	$88.9e^{-0.1t} + 17.4e^{-1.0t} - 25.0e^{-0.8t} - 81.2e^{-0.2t}$
dC_{3comp}/dt	$139e^{-2t} + 312e^{-1.0t} - 233e^{-0.8t} - 18.1e^{-0.2t}$	$-8.89e^{-0.1t} - 17.4e^{-1.0t} + 20.0e^{-0.8t} + 16.2e^{-0.2t}$
d^2C_{3comp}/dt^2	$-278e^{-2t} - 312e^{-1.0t} + 187e^{-0.8t} + 3.61e^{-0.2t}$	$0.889e^{-0.1t} + 17.4e^{-1.0t} - 16.0e^{-0.8t} - 3.25e^{-0.2t}$
$T_{max,3comp,true}$ (h)	1.28	6.45
$C_{max,3comp,true}$ (µg/mL)	82.4	24.2
Multi-Compartment, oral (τ =6; parameters same as above; k_a = 2 h^{-1})		
	2 Compartment (Fast Absorption)	**3 Compartment (Fast Absorption)**
C_{multi}	$-139e^{-2t} + 84.0e^{-0.8t} + 79.6e^{-0.2t}$	$-69.4e^{-2t} - 313e^{-1.0t} + 294e^{-0.8t} + 129e^{-0.2t}$
dC_{multi}/du	$278e^{-2t} - 67.2e^{-0.8t} - 15.9e^{-0.2t}$	$139e^{-2t} + 313e^{-1.0t} - 235e^{-0.8t} - 25.8e^{-0.2t}$
d^2C_{multi}/du^2	$-556e^{-2t} + 53.8e^{-0.8t} + 3.18e^{-0.2t}$	$-278e^{-2t} - 313e^{-1.0t} + 188e^{-0.8t} + 5.17e^{-0.2t}$
$T_{max,multi,true}$ (h)	0.899	1.13
$C_{max,multi,true}$ (µg/mL)	84.3	114

Table 2. Effects of varying k_a on estimates of T_{max} and C_{max} from simulated blood data, which contained 5% assay error. Values assigned were: $\alpha,\ \beta,\ and\ k_{21} =$ 0.8, 0.2, and 0.5 h^{-1}, respectively.

	True Value	**2 Compartment Model**			**Observed Values (FDA method)**		
k_a (h^{-1})	**$T_{max,true}$ (h)**	**$T_{max,2comp}$ (h)**	**%Bias[a]**	**RSD[b]**	**$T_{max,obs}$ (h)**	**%Bias**	**RSD**
3	0.743	0.744	0.181%	5.67%	0.782	5.28%	20.4%
2	0.972	0.971	-0.0257%	4.62%	0.947	-2.58%	19.9%
1	1.51	1.52	0.310%	3.85%	1.62	7.36%	19.1%
0.1	5.77	5.75	-0.351%	5.08%	6.01	4.01%	21.1%
0.05	8.07	7.97	-1.17%	5.78%	7.93	-1.69%	23.0%
k_a (h^{-1})	**$C_{max,true}$ (µg/mL)**	**$C_{max,2comp}$ (µg/mL)**	**%Bias**	**RSD**	**$C_{max,obs}$ (µg/mL)**	**%Bias**	**RSD**
3	70.7	70.9	0.222%	2.54%	72.1	2.04%	3.76%
2	64.2	64.1	-0.0779%	2.49%	65.3	1.74%	3.98%
1	51.9	51.8	-0.0675%	2.19%	52.8	1.76%	3.90%
0.1	16.3	16.3	0.338%	2.62%	16.6	2.00%	3.76%
0.05	10.0	10.1	0.169%	2.69%	10.2	2.09%	3.81%

[a] %Bias was determined using Eq. 12.
[b] RSD was determined using Eq. 13.

DMD Fast Forward. Published on August 22, 2018 as DOI: 10.1124/dmd.118.082636
This article has not been copyedited and formatted. The final version may differ from this version.

Figure 1

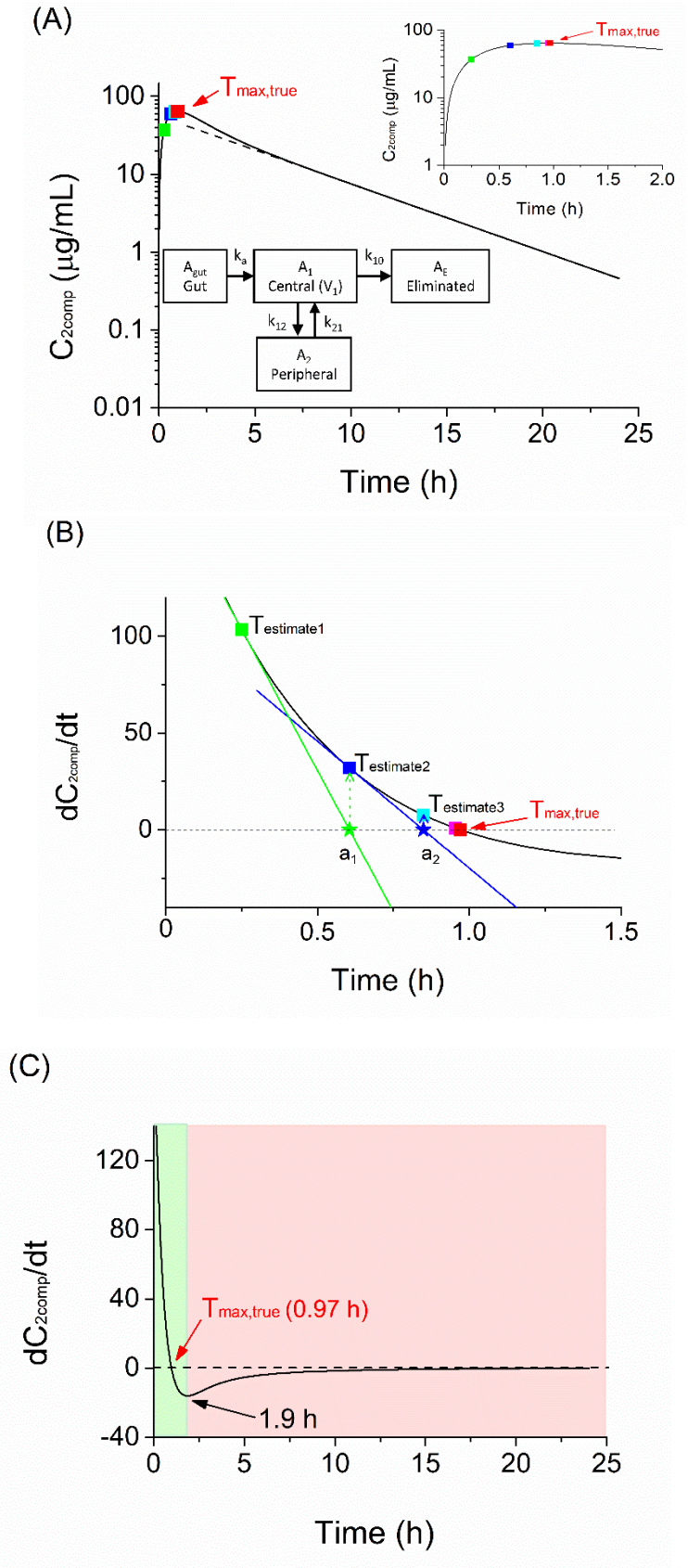

DMD Fast Forward. Published on August 22, 2018 as DOI: 10.1124/dmd.118.082636
This article has not been copyedited and formatted. The final version may differ from this version.

Figure 2

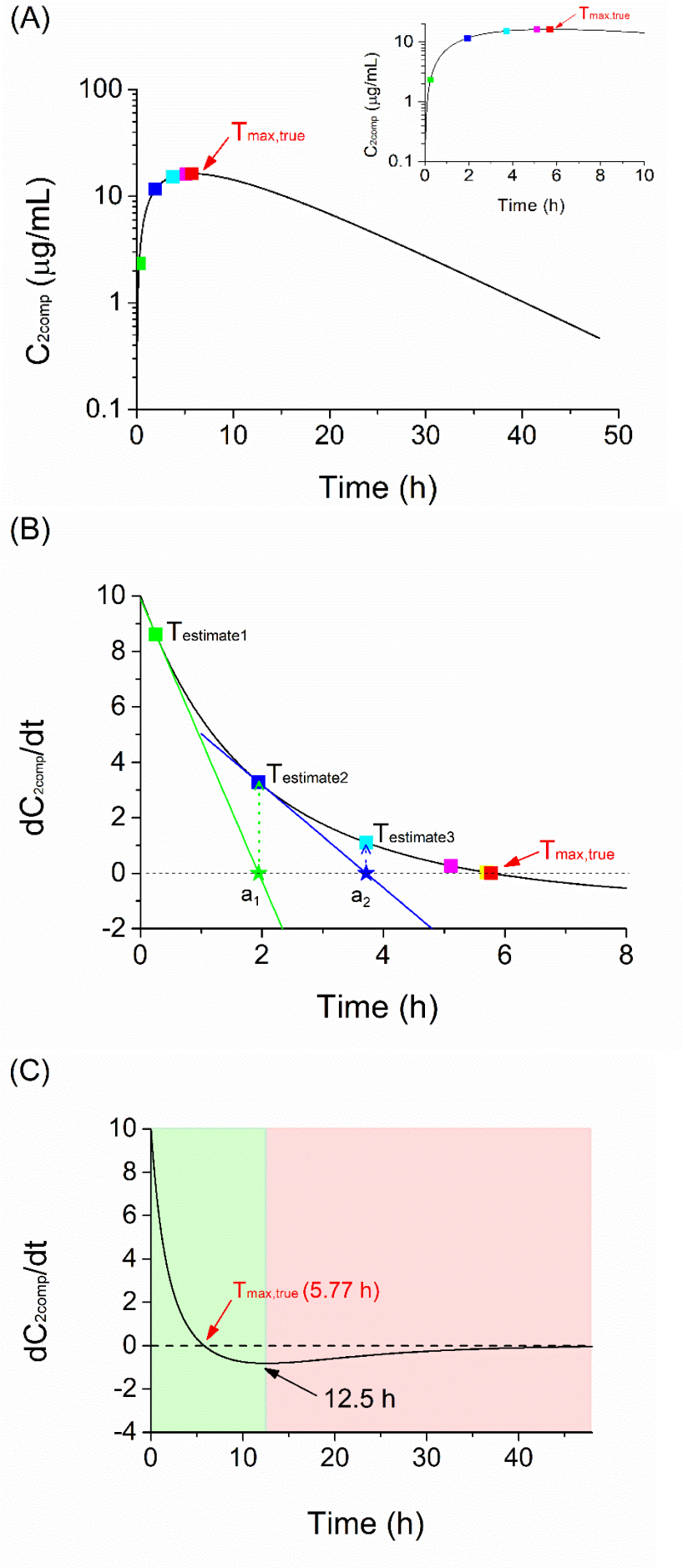

Figure 3

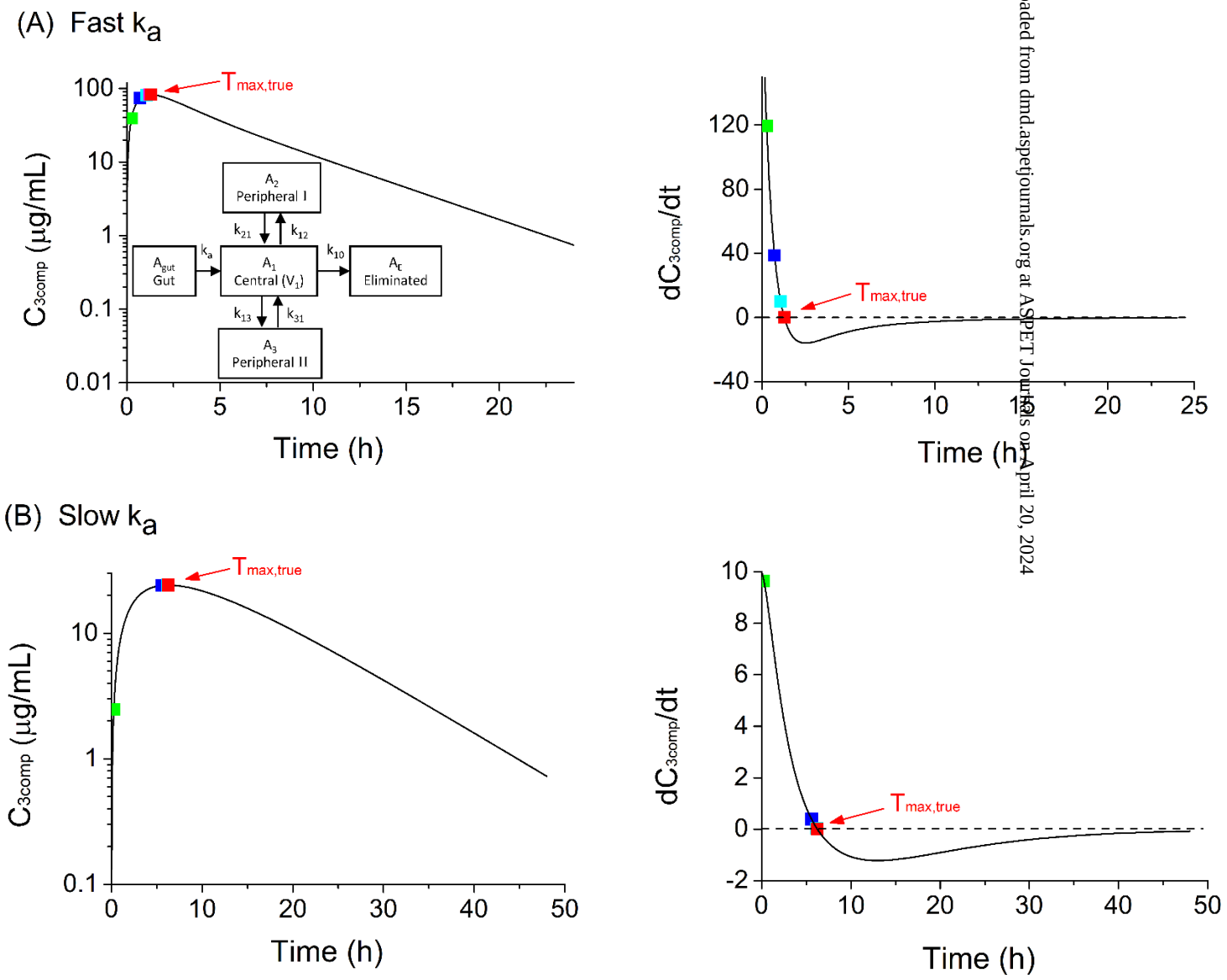

Figure 4

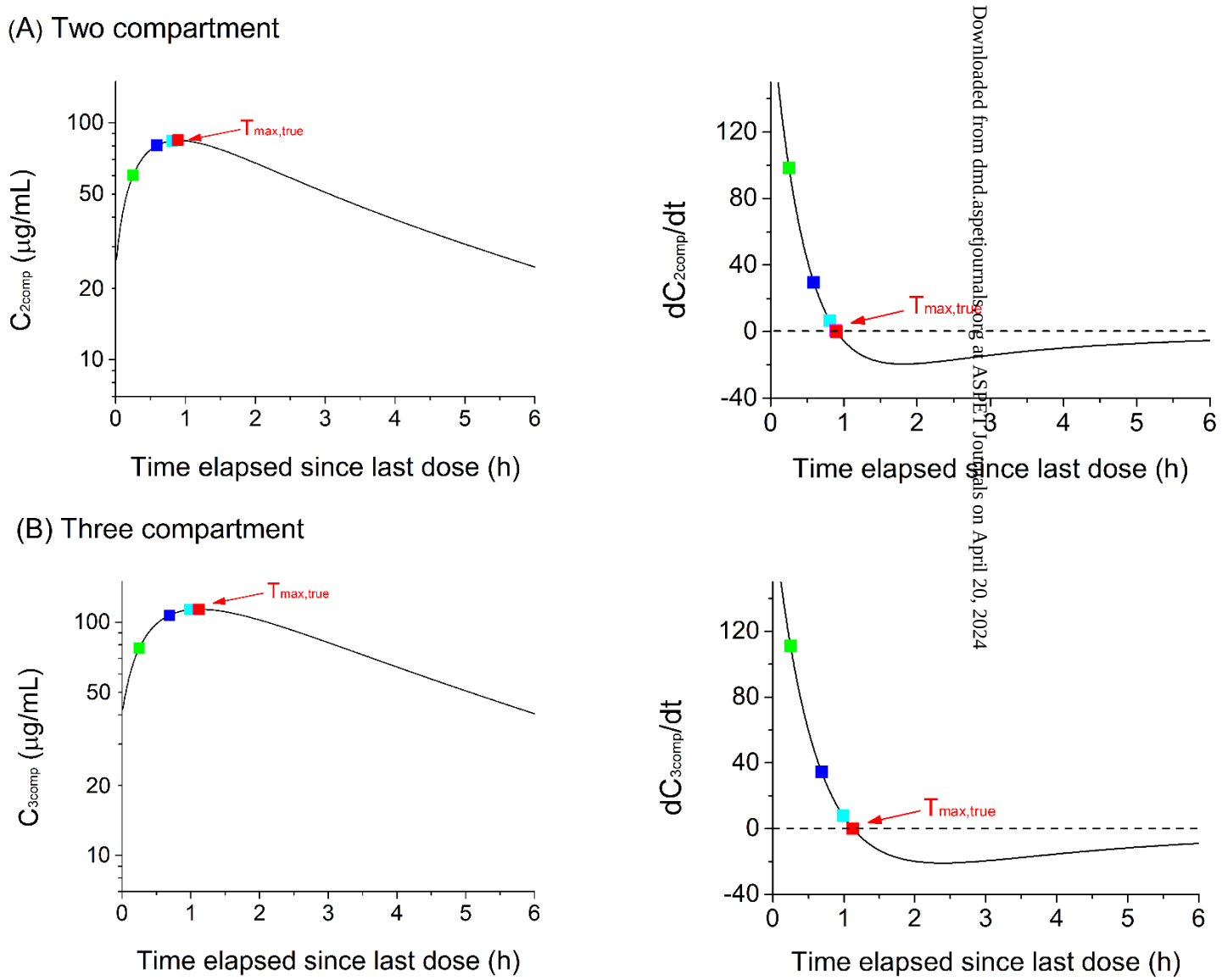

Figure 5

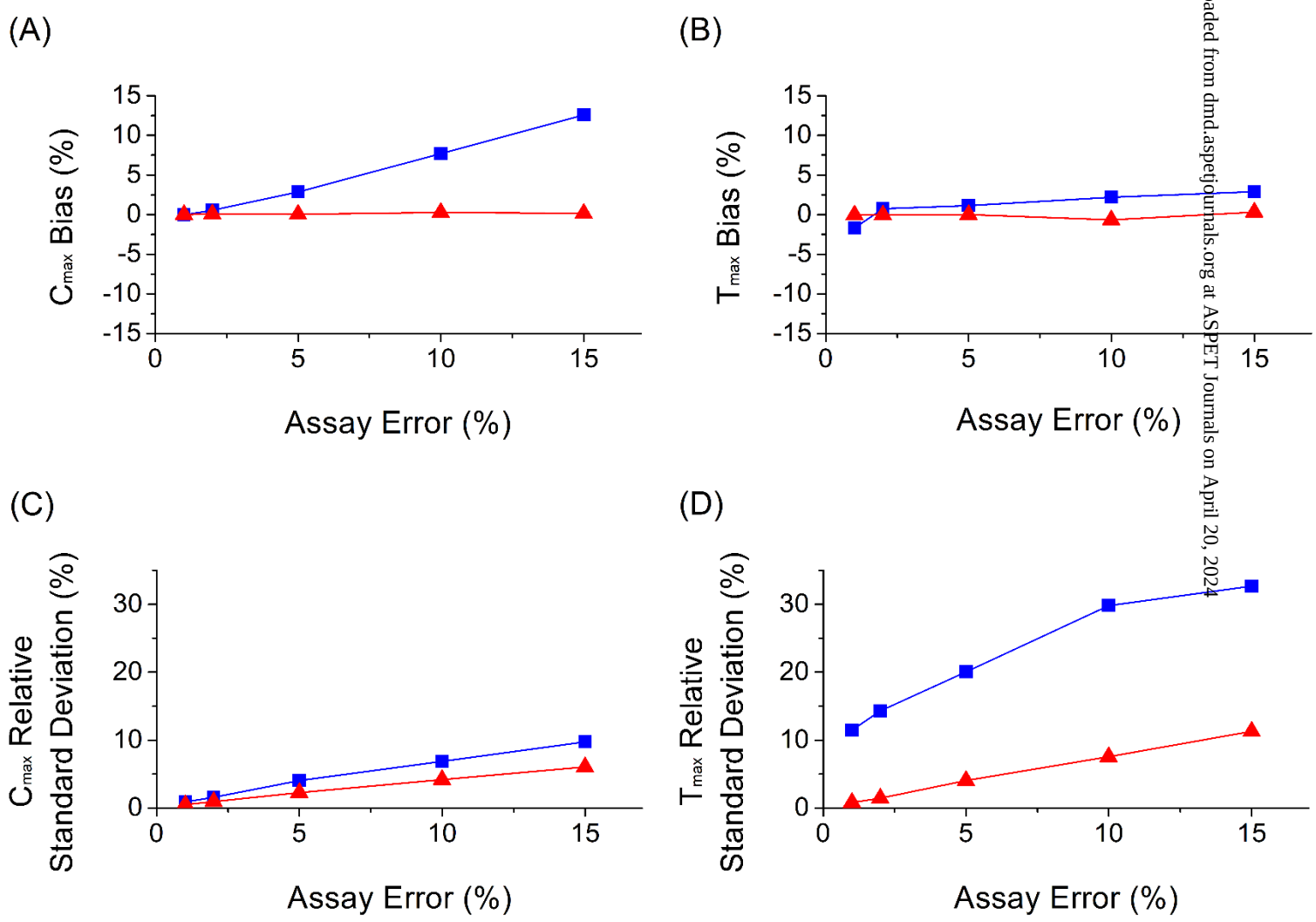

Figure 6